

The Binding Interactions between Cyclohexanocucurbit[6]uril and Alkyl Viologens Give Rise to a Range of Diverse Structures in the Solid and the Solution Phases

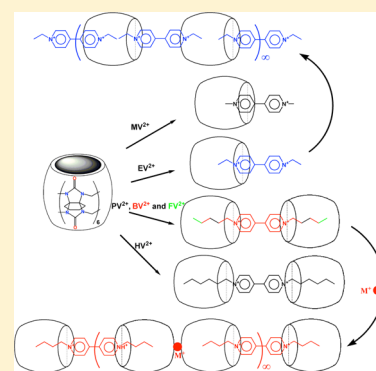
Rui-Lian Lin,[†] Jia-Qing Li,[‡] Jing-Xin Liu,^{*,†} and Angel E. Kaifer^{*,‡}

[†]College of Chemistry and Chemical Engineering, Anhui University of Technology, Maanshan 243001, China

[‡]Center for Supramolecular Science and Department of Chemistry, University of Miami, Coral Gables, Florida 33124-0431, United States

S Supporting Information

ABSTRACT: The binding interactions between the cyclohexanocucurbit[6]uril (Cy6CB6) host and a series of dialkyl-4,4'-bipyridinium (viologen) dicationic guests were investigated in the solution phase, using ¹H NMR spectroscopy, and in the solid phase, using X-ray diffraction methods. In D₂O solution, methyl viologen (MV²⁺) and ethyl viologen (EV²⁺) form 1:1 complexes in which the bipyridinium aromatic nucleus is partially included inside the Cy6CB6 cavity. Propyl viologen (PV²⁺), butyl viologen (BV²⁺), pentyl viologen (FV²⁺), and heptyl viologen (HV²⁺) form 2:1 complexes with Cy6CB6, in which each of the viologen aliphatic chains is included by a host molecule. In the solid state, EV²⁺ forms a polypseudorotaxane via pseudorotaxane interdigitation of Cy6CB6 hosts. The PV²⁺ guest forms a dumbbell-shaped structure with a Cy6CB6 host residing over each of the terminal propyl groups of the guest. In contrast to this, the BV²⁺ guest and Cy6CB6 form a different polypseudorotaxane structure in which dumbbell-shaped structures, formed by two host molecules interacting with a single guest, are interconnected through metal–host coordination.

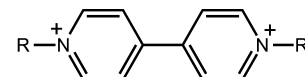
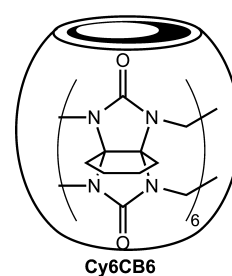


INTRODUCTION

The family of cucurbit[*n*]uril receptors^{1–8} has attracted a lot of interest in the last 15 years because of their exceptional binding properties with suitable guests in aqueous media. While cucurbit[7]uril (CB7) is soluble in aqueous solution to millimolar levels, cucurbit[6]uril (CB6) and cucurbit[8]uril (CB8) are considerably less soluble in water.² Interestingly, CB6 derivatives with aliphatic equatorial substituents, such as tetramethylcucurbit[6]uril⁹ (Me₄CB6), exhibit higher water solubility than CB6 itself. This is also the case with cyclohexanocucurbit[6]uril (Cy6CB6), a host whose binding properties are the subject of current interest by several groups.^{10–12}

The class of 4,4'-bipyridinium derivatives (viologens) are well-known guests for the cucurbit[*n*]uril hosts. Methyl viologen was one of the first guests investigated for inclusion by the CB7 host,^{13,14} and a number of viologens^{15,16} and related pyridinium derivatives¹⁷ have been investigated as guests for CB6 and its derivatives. Isaacs has used the binding interactions between a dimeric CB6 and oligomeric viologens to assemble fascinating examples of supramolecular ladder structures.¹⁸ While the cavity of CB7 is wide enough to include the bipyridinium residue of viologens,^{13,14} CB6 and its derivatives have narrower cavities, which usually cannot accommodate the bipyridinium residue in its entirety. Therefore, we decided to investigate the binding interactions in aqueous solution between Cy6CB6 and a series of simple alkyl-

N,N'-bipyridinium (alkyl viologens) shown in Figure 1. We also expanded our investigation to the solid state, since we could



MV²⁺, R = CH₃
 EV²⁺, R = CH₂CH₃
 PV²⁺, R = CH₂CH₂CH₃
 BV²⁺, R = CH₂CH₂CH₂CH₃
 FV²⁺, R = CH₂CH₂CH₂CH₂CH₃
 HV²⁺, R = CH₂CH₂CH₂CH₂CH₂CH₂CH₃
Viologen Guests

Figure 1. Structures of the Cy6CB6 host and the viologen guests used in this work.

solve the crystal structures of some of the Cy6CB6–viologen complexes surveyed in this work. The results of this research work are described here.

RESULTS AND DISCUSSION

NMR Spectroscopic Data in the Solution Phase. The binding interactions between the viologen guests and Cy6CB6 were monitored using ¹H NMR spectroscopic data recorded in

Received: July 7, 2015

Published: October 9, 2015

neutral D₂O solution. Figure 2 shows the changes observed in the spectrum of MV²⁺ as progressively larger amounts of

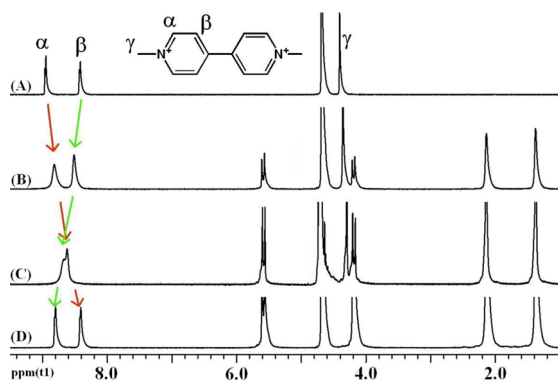


Figure 2. ¹H NMR spectra (400 MHz, D₂O) of MV²⁺ (A) in the absence and in the presence of (B) 0.25, (C) 0.48, and (D) 1.01 equiv of Cy6CB6 in D₂O at 20 °C.

Cy6CB6 are added to the solution. As the concentration of Cy6CB6 increases, the signal corresponding to the α aromatic protons of the guest shifts upfield and that for the β protons shifts downfield. The relative position of both signals is inverted upon addition of ca. 1.0 equiv of Cy6CB6 in relation to the original signal positions in the free guest. The signal corresponding to the methyl protons (labeled γ in the figure) also shifts upfield, but the magnitude of its complexation-induced shift is less pronounced than that experienced by the α protons signal. Upon addition of 1 equiv of host, the α protons signal shifts upfield by 0.52 ppm, while the methyl protons signal shifts only 0.28 ppm. The complexation-induced shift of the signal for the β protons is 0.45 ppm at the same point in the titration with Cy6CB6. At each concentration of Cy6CB6, we only observed a single set of signals for the guest, which reveals that the guest exchange is fast compared to the NMR time scale. These data indicate that part of MV²⁺ is inserted into the cavity of Cy6CB6, forming a 1:1 inclusion complex in which one of the positively charged nitrogens in the viologen nucleus is included in the cavity. Since the guest exchange is fast, the symmetry of the guest is maintained in the NMR spectra and both ends of the viologen remain equivalent. The structure of this complex is similar to that observed by Sindelar and co-workers, between a derivative of CB6 and MV²⁺,¹⁵ and by Wei et al, between Me4CB6 and MV²⁺.¹⁶

The binding behavior between Cy6CB6 and EV²⁺ is illustrated by the ¹H NMR spectra shown in Figure 3. While the overall behavior seems at first glance similar to that observed with MV²⁺, close inspection reveals some differences. First, the complexation-induced shift for the signal corresponding to the α aromatic protons of EV²⁺ (0.33 ppm) is smaller than that observed for MV²⁺ (0.52 ppm). In the case of EV²⁺, the addition of 1 equiv of the host is not enough to invert the relative positions of the α and β proton signals, unlike in the case of MV²⁺. The two aliphatic proton signals (labeled γ and δ in the figure) also respond to the presence of the host with small upfield shifts. As in the case of MV²⁺, the chemical exchange between free EV²⁺ and its Cy6CB6 complex is fast in relation to the NMR time scale.

To further investigate the formation of the complexes between Cy6CB6 and these two viologen guests, we first carried out NMR titrations, monitoring the chemical shift of key proton signals on the guest as a function of increasing host

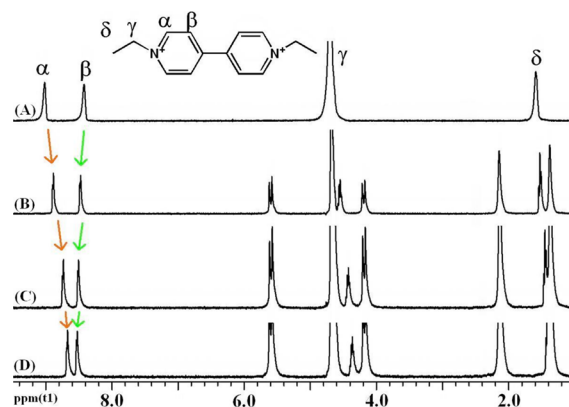


Figure 3. ¹H NMR spectra (400 MHz, D₂O) of guest EV²⁺ (A) in the absence and in the presence of (B) 0.42, (C) 0.82, and (D) 1.10 equiv of Cy6CB6 in D₂O at 20 °C.

concentration. However, these plots lack curvature, indicating that the equilibrium association constants (K) are larger than the range of values typically accessible in these NMR experiments. To obtain the corresponding K values, we carried out isothermal titration calorimetry (ITC) experiments (Figure 4). The K values obtained were $(1.7 \pm 0.2) \times 10^5$ and $(4.8 \pm 0.5) \times 10^4 \text{ M}^{-1}$, for the Cy6CB6·MV²⁺ and Cy6CB6·EV²⁺ complexes, respectively, which are about 1 order of magnitude lower than the value recorded in the literature for the complex formed between MV²⁺ and an hexamethylated derivative of CB6,¹⁵ but similar to the reported K value for the complex between EV²⁺ and Me4CB6.¹⁶ Table 1 gives all the thermodynamic parameters obtained for these two complexes in our ITC experiments.

As shown in Figure 5a, the binding behavior of Cy6CB6 with guest PV²⁺ clearly departs from our observations with MV²⁺ and EV²⁺. Upon addition of the host, all the proton resonances corresponding to the aliphatic propyl chains undergo upfield shifts. The signal for the α aromatic protons shifts downfield, while the signal for the β protons does not show any significant changes. This behavior can be rationalized by the inclusion of the propyl chain inside the cavity of the host, with the bipyridinium nucleus remaining outside. Only a single set of proton resonances is observed as the concentration of Cy6CB6 increases, revealing that the chemical exchange between the guest and the Cy6CB6 complex is in the fast regime compared to the NMR time scale. The chemical shift of the α aromatic protons of PV²⁺ as a function of the Cy6CB6 concentration clearly levels off at 2.0 equiv of added host (Figure 5b), suggesting a 2:1 (host/guest) stoichiometry for the complex, which we can formulate as (Cy6CB6)₂·PV²⁺.

Figure 6 clearly shows that the changes induced by Cy6CB6 on the ¹H NMR spectra of BV²⁺ and FV²⁺ are similar; both guests feature a similar mode of binding interactions with the host. The NMR data show the simultaneous observation of sets of peaks for the complex and the free guest as long as [Cy6CB6] < 2[guest]. Once 2.0 equiv of Cy6CB6 are added, only the set of peaks corresponding to the complex is observed. The upfield shifts observed for all the aliphatic proton resonances strongly indicate that the preferred binding sites for Cy6CB6 are the terminal aliphatic chains. The signal for the β aromatic protons is not significantly shifted, while the signal for the α aromatic protons experiences a downfield shift. These two findings are consistent with the viologen nucleus remaining outside of the host cavity. All these experimental observations

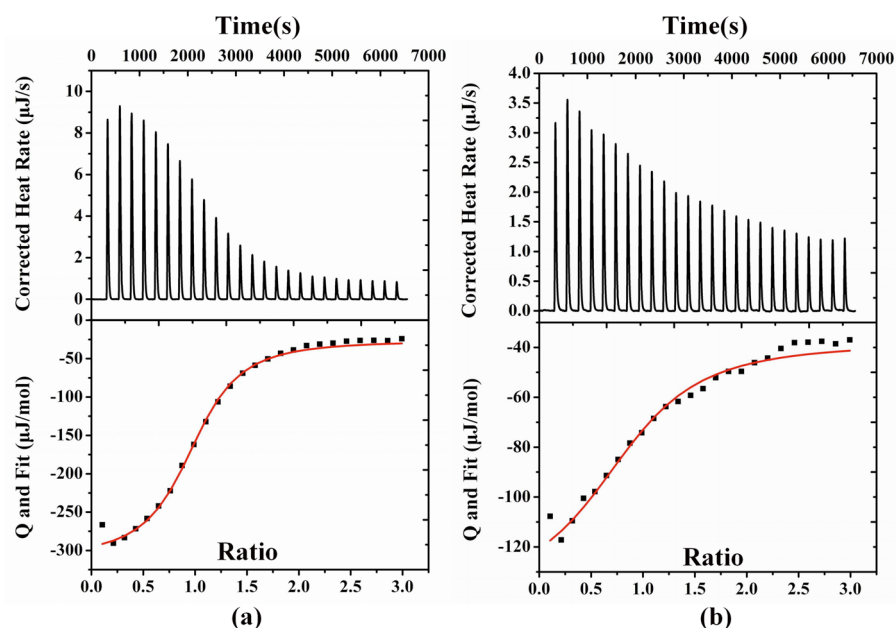


Figure 4. ITC profiles for the Cy6CB6 complexation with (a) guest MV^{2+} and (b) guest EV^{2+} at 298.15 K.

Table 1. Thermodynamic Parameters Obtained by ITC for the Cy6CB6 Complexation of MV^{2+} and EV^{2+} in Aqueous Media at 25 °C

complex	K, M^{-1}	$\Delta G^\circ, kJ mol^{-1}$	$\Delta H^\circ, kJ mol^{-1}$	$T\Delta S^\circ, kJ mol^{-1}$
Cy6CB6- MV^{2+}	$(1.7 \pm 0.2) \times 10^5$	-29.9	-28.3	1.6
Cy6CB6- EV^{2+}	$(4.8 \pm 0.5) \times 10^4$	-26.7	-10.0	16.7

indicate the formation of a 2:1 host–guest inclusion complex with two Cy6CB6 molecules residing on the aliphatic (butyl for BV^{2+} or pentyl for FV^{2+}) chains. It is noteworthy that a single methylene addition to each of the propyl chains in PV^{2+} is enough to slow down the complex dissociation kinetics from the fast to the slow regime in the NMR time scale.

1H NMR spectroscopy was also used to monitor the binding behavior of Cy6CB6 with the last guest in the series, HV^{2+} . In the presence of various concentrations of Cy6CB6 (Figure 7), the chemical shifts for all the protons on HV^{2+} are very similar to those observed in the case of BV^{2+} . The only difference is that no significant change is observed in the chemical shift for

the methylene protons adjacent to the quaternary nitrogens (N^+-CH_2-) on the viologen group (γ protons), suggesting that the corresponding carbon atoms are located very close to the center of the Cy6CB6 portal.

It should be noted here that even with a [guest]/[host] ratio higher than 2.0, only one set of signals was observed in the case of the first three guests (MV^{2+} , EV^{2+} , and PV^{2+}), suggesting that the chemical exchange between the free and the bound guests is relatively fast on the NMR time scale. As stated before, in the case of the other three guests (BV^{2+} , FV^{2+} , and HV^{2+}), the 1H NMR signals of free and bound guests were distinguishable in the spectra when less than 2.0 equiv of Cy6CB6 was added, indicating that the exchange rate between bound and free viologen guest is slow on the 1H NMR time scale.

It is evident that one of the major driving forces for the formation of these complexes is the ion–dipole interactions between the positively charged nitrogens on the guest and the oxygen atoms on the portals of Cy6CB6. However, the actual binding site (Scheme 1) depends strongly on the length of the terminal aliphatic chains because the hydrophobic interactions

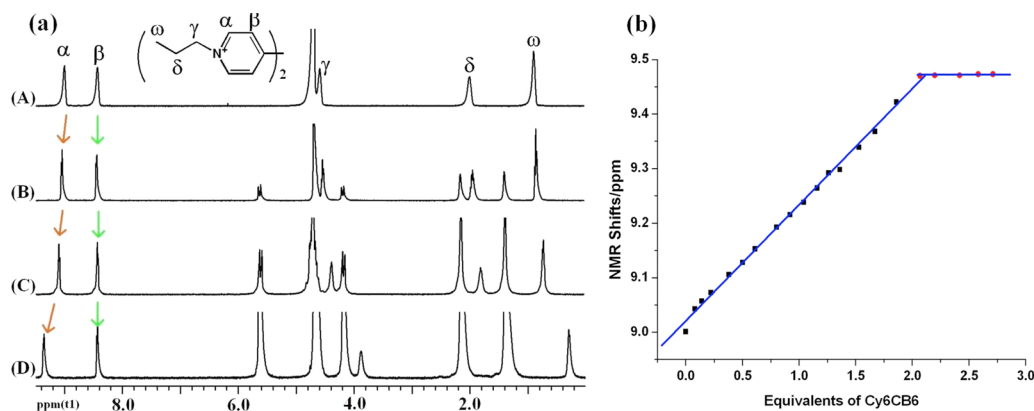


Figure 5. (a) 1H NMR spectra (400 MHz, D_2O) of guest PV^{2+} (A) in the absence and in the presence of (B) 0.15, (C) 0.38, and (D) 1.67 equiv of Cy6CB6; (b) 1H NMR chemical shift of the α aromatic protons of PV^{2+} as a function of the added concentration of Cy6CB6.

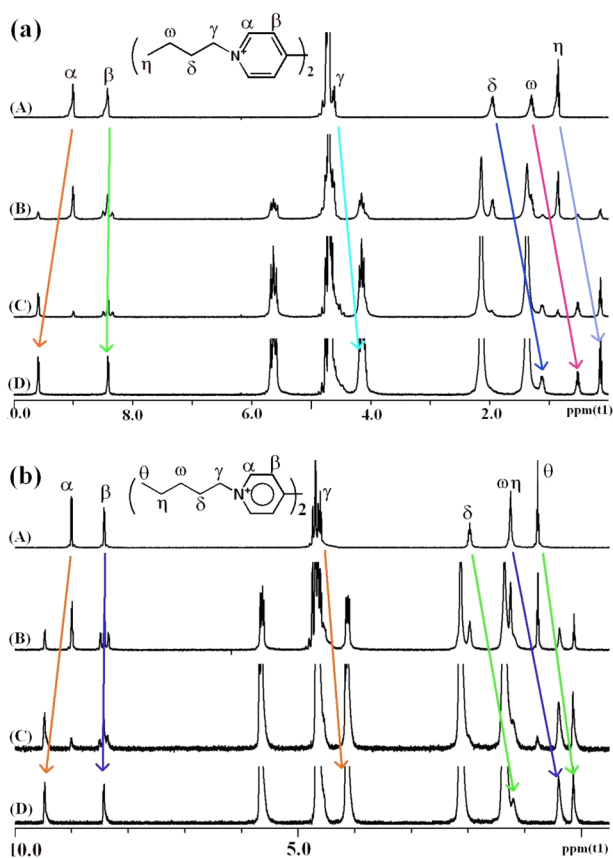


Figure 6. (a) ^1H NMR spectra (400 MHz, D_2O) of guest BV^{2+} (A) in the absence and in the presence of (B) 0.42, (C) 1.72, and (D) 2.50 equiv of Cy6CB6 in D_2O at 20 °C; (b) ^1H NMR spectra (400 MHz, D_2O) of guest FV^{2+} (A) in the absence and in the presence of (B) 0.62, (C) 1.40, and (D) 2.20 equiv of Cy6CB6 in D_2O at 20 °C.

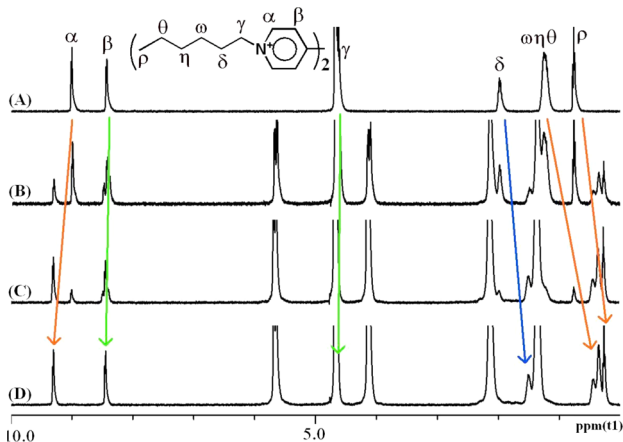
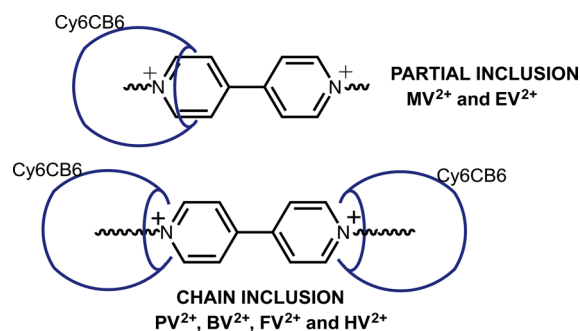


Figure 7. ^1H NMR spectra (400 MHz, D_2O) of guest HV^{2+} (A) in the absence and (B) in the presence of (B) 0.62, (C) 1.64, and (D) 2.13 equiv of Cy6CB6 in D_2O at 20 °C.

between the guest's chains and the inner cavity of Cy6CB6 also play an important role in the complexation process. For the viologen guests with short chains (MV^{2+} and EV^{2+}), the methyl group and the ethyl group, respectively, cannot develop significant hydrophobic interactions with Cy6CB6. Therefore, the short aliphatic chains, as well as part of the bipyridinium moiety, are engulfed into the cavity of Cy6CB6, forming 1:1 binary inclusion complexes. In the case of viologen guests with

Scheme 1. Two Basic Modes of Binding Interactions between the Surveyed Viologen Guests and Cy6CB6



longer chains (PV^{2+} , BV^{2+} , FV^{2+} , and HV^{2+}), only the aliphatic chains are included into the cavity of Cy6CB6 due to the favorable hydrophobic interactions between the host cavity and the terminal aliphatic chain, forming 2:1 ternary complexes, since two host molecules can interact with a single guest molecule. The finding that the aliphatic chain is more favorably encapsulated into the hydrophobic cavity than the aromatic group can be exploited for the design and synthesis of polypseudorotaxanes and other supramolecular polymers.

We must note that there are minor differences in the extent of penetration of the guest through the host cavity in the complexes formed by the guests MV^{2+} and EV^{2+} . On the basis of the NMR data, the ethyl group seems to limit slightly how much the bipyridinium group penetrates into the host cavity as compared to the complex with MV^{2+} . Similarly, in the complex with HV^{2+} , the hosts are not as close to the positively charged nitrogens as they are in the complexes with PV^{2+} , BV^{2+} , and FV^{2+} . In spite of these minor differences, it is clear that all the Cy6CB6 complexes investigated here fall within the two classes represented in Scheme 1. Our group reported a similar investigation of the binding interactions between CB7 and the same series of viologens.¹⁹ The results are strongly related to our findings in this work, as the CB7 complexes also fall into two classes. The first class consists of complexes in which CB7 is fully centered on the bipyridinium nucleus, and the second class corresponds to complexes in which the CB7 hosts interact with the terminal aliphatic chains. In the case of the CB7 host, the first class of complexes is formed by MV^{2+} and EV^{2+} , with BV^{2+} , FV^{2+} and HV^{2+} giving rise to the second class. PV^{2+} was found to be an intermediate case with CB7. In any instance, the similarities between the binding interactions of this series of viologen guests with the two hosts, CB7 and Cy6CB6, are remarkable. The only significant difference derives from the smaller cavity of Cy6CB6, which is not wide enough to fully encapsulate the viologen nucleus.

X-ray Diffraction Data in the Solid State. We also investigated the structure of these inclusion complexes in the solid state. Good quality single crystals of two of the inclusion complexes $\text{Cy6CB6}\cdot\text{EV}^{2+}$ (compound 1) and $\text{Cy6CB6}\cdot\text{PV}^{2+}$ (compound 2) were successfully obtained by slow vapor evaporation of aqueous solutions containing the Cy6CB6 host and the corresponding viologen guest. Single-crystal X-ray diffraction analysis reveals that both compounds (1 and 2) crystallized in the triclinic system with the $P\bar{1}$ space group. In the solid state, Cy6CB6 host and EV^{2+} guest display a unique binding mode, which is distinctly different from that in aqueous solution. As shown in Figure 8, both ethyl groups of each EV^{2+} guest are engulfed into the cavities of two Cy6CB6 hosts, while

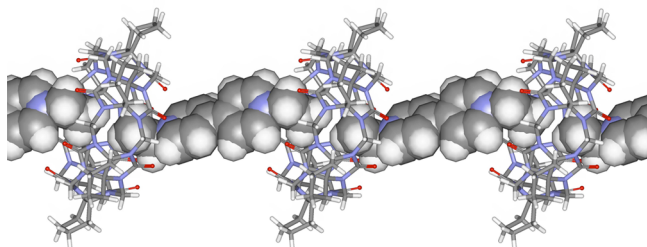


Figure 8. Polypseudorotaxane structures observed in the crystal structure of solid **1** (Cy6CB6-EV²⁺). Atomic color code: O = red, C = gray, N = light blue, and H = white.

the whole viologen nucleus resides outside of the portal of the Cy6CB6. Each Cy6CB6 host, on the other hand, includes two ethyl groups from two EV²⁺ guests. As a result, the EV²⁺ guests and Cy6CB6 hosts form a polypseudorotaxane through pseudorotaxane interdigitation of the hosts. In the crystal structure of compound **1**, the polypseudorotaxane is aligned parallel to the *b*-axis and each polypseudorotaxane is surrounded by numerous water molecules and bromide counteranions. It is noteworthy that the solid-state structure of this complex is different from that reported for the complex between the same guest and the related host, Me4CB6.

The structure of solid compound **2** is shown in Figure 9. Both propyl groups of each PV²⁺ guest are inserted into the

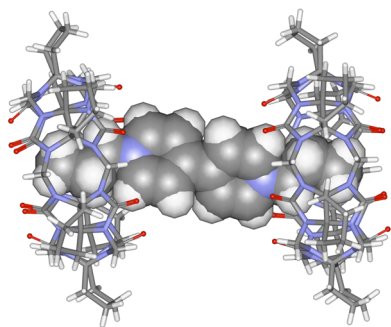


Figure 9. Dumbbell-shaped complex observed in the crystal structure of solid compound **2** (formed between Cy6CB6 and PV²⁺). Atomic color code: O = red, C = gray, N = light blue, and H = white.

cavities of two Cy6CB6 hosts, forming a dumbbell-shaped structure, which is in agreement with their ¹H NMR spectroscopic data in D₂O solution. Obviously, the formation of polypseudorotaxanes in compound **1** and dumbbell-shaped structures in compound **2** is attributed to strong host–guest interactions, including charge–dipole interactions between the guest and the carbonyl oxygens on the portals of the Cy6CB6 host and the hydrophobic interactions between the alkyl chain and the inner wall of the Cy6CB6 cavity.

According to our ¹H NMR spectroscopic data, we reasoned that guest BV²⁺ would also form a dumbbell-shaped structure with Cy6CB6 similar to that observed in solid compound **2** because the host cavity is large enough to encapsulate only one butyl group and supramolecular polymerization, similar to that seen in the structure of solid compound **1**, cannot occur. We were intrigued by the possibility of using metal coordination to create connections between neighboring dumbbell-shaped structures. Addition of BV²⁺ to Cy6CB6 in the presence of potassium ions resulted in the formation of the potassium-bridged solid compound **3**. X-ray crystallography confirms that

compound **3** crystallizes in the triclinic system, also with space group *P*1̄. As seen in Figure 10, both butyl groups of the guest

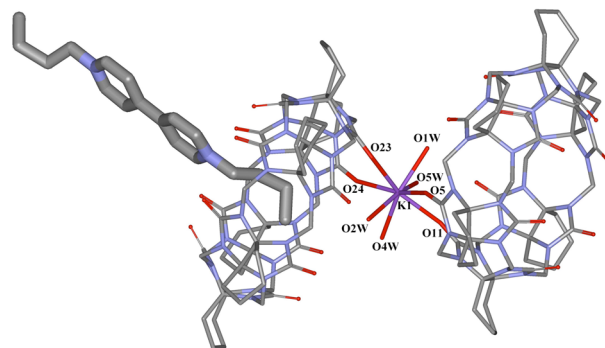


Figure 10. Structure observed in solid compound **3** showing the contorted conformation of the butyl chains of the guest and the potassium ion coordination environment. Solvation water molecules and chloride anions are omitted for clarity. Atomic color code: O = red, C = gray, N = light blue, and H = white.

reside in the cavity of the Cy6CB6 hosts, in similar fashion to compound **2**. The butyl group is expected to adopt an extended conformation when bound within the cavity of the Cy6CB6 host. However, close inspection reveals that both butyl groups exhibit a contorted conformation. We also observed that there is only one crystallographically independent K(I) center in an asymmetric unit of compound **3**. Each K(I) is octa-coordinated to two bidentate Cy6CB6 hosts, with a mean K–O distance of 2.427 Å, and to four water molecules, with a mean K–O distance of 2.456 Å. Owing to the bridging behavior of the K(I) ion, the neighboring dumbbell-shaped structures are connected to form a novel 1D polypseudorotaxane (Figure 11), which combines host–guest and metal–host interactions. Further analysis of the extended solid-state structure shows that the polypseudorotaxanes are associated with channels (viewing

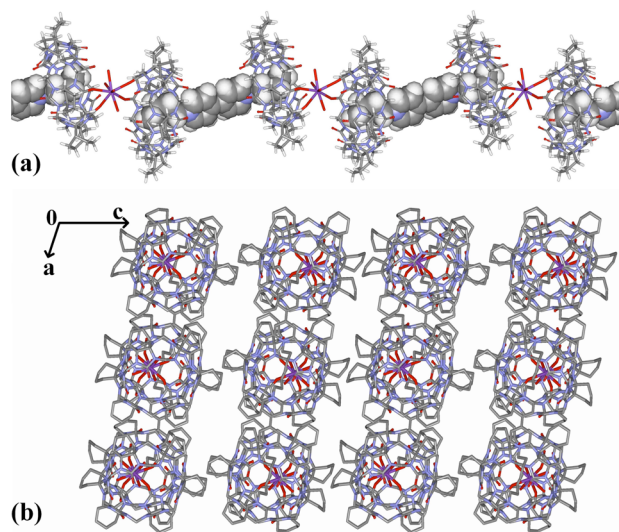


Figure 11. (a) Polypseudorotaxane structures observed in solid compound **3**; (b) packing diagram of compound **3** viewed down the *b*-axis (on *ac* plane). Anions and solvation water molecules are omitted for clarity. Atomic color code: O = red, C = gray, N = light blue, and H = white.

down the *b*-axis) occupied by chloride and bromide anions and water molecules.

CONCLUSIONS

In summary, we have investigated the binding interactions of Cy6CB6 with a series of dialkyl-viologen dicationic guests using ^1H NMR spectroscopy and X-ray crystallography. In aqueous solution (D_2O), the aromatic nuclei of MV^{2+} and EV^{2+} were partially encapsulated into the Cy6CB6 host, giving rise to 1:1 binary inclusion complexes. In contrast to this finding, with the longer chain viologens (PV^{2+} , BV^{2+} , FV^{2+} , and HV^{2+}), only the alkyl chains were engulfed into the cavity of the Cy6CB6 host, forming 2:1 ternary complexes. These findings suggest that the inclusion of the aliphatic chains is favored compared to inclusion of the aromatic bipyridinium group. In the solid state, the EV^{2+} and PV^{2+} guests form a polypseudorotaxane and a dumbbell-shaped structure, respectively, with Cy6CB6. In the presence of KCl, BV^{2+} guests form a different polypseudorotaxane with Cy6CB6 hosts, taking advantage of combined host–guest and metal–host interactions. The solid-state structures of these complexes show a number of interesting and differential features, not only as compared to the same complexes in solution, but also compared to similar viologen complexes formed by related hosts, such as Me4CB6.

EXPERIMENTAL SECTION

Starting materials and solvents for syntheses were commercially available and used as supplied without further purification. Cy6CB6 was prepared by the method of Kim and co-workers.¹⁰ With the exception of methyl viologen, which is commercially available, all other guests were straightforwardly prepared by the treatment of 4,4'-bipyridine with excess of the corresponding bromoalkane.¹⁹ The C, H, and N microanalyses were carried out with an elemental analyzer.

Preparation of Compound 1. Cy6CB6·12H₂O (0.078 g, 0.05 mmol) and *N,N'*-diethyl-4,4'-bipyridinium dibromide ($\text{EV}^{2+}\cdot 2\text{Br}^-$, 0.018 g, 0.05 mmol) were dissolved in water (5 mL). The mixture was heated at 50 °C for 10 min. After cooling to room temperature, the mixture was filtered. Slow evaporation of the filtrate over a period of 2 weeks provided colorless crystals. Yield: 0.047 g (60% based on Cy6CB6). Anal. Calcd for $(\text{C}_{60}\text{H}_{72}\text{N}_{24}\text{O}_{12})\cdot(\text{C}_{14}\text{N}_2\text{H}_{18})\cdot 2\text{Br}\cdot 6\text{H}_2\text{O}$ (1): C, 49.28; H, 5.70; N, 20.19. Found: C, 49.17; H, 5.75; N, 20.16.

Preparation of Compound 2. Solid compound 2 was obtained following the method described above for compound 1. Yield: 0.043 g (55% based on Cy6CB6). Anal. Calcd for $(\text{C}_{60}\text{H}_{72}\text{N}_{24}\text{O}_{12})_2\cdot(\text{C}_{16}\text{N}_2\text{H}_{22})\cdot 2\text{Br}\cdot 31\text{H}_2\text{O}$ (2): C, 45.33; H, 6.38; N, 19.44. Found: C, 45.37; H, 6.35; N, 19.46.

Preparation of Compound 3. To a solution of Cy6CB6·12H₂O (0.078 g, 0.05 mmol) in HCl (1 mol·L⁻¹, 5 mL) were added KCl (0.0019 g, 0.025 mmol) and *N,N'*-butyl-4,4'-bipyridinium dibromide ($\text{BV}^{2+}\cdot 2\text{Br}^-$, 0.022 g, 0.05 mmol). Yield: 0.023 g (30% based on Cy6CB6). Anal. Calcd for $[\text{K}(\text{H}_2\text{O})_4(\text{C}_{60}\text{H}_{72}\text{N}_{24}\text{O}_{12})_2]\cdot(\text{C}_{18}\text{N}_2\text{H}_{26})\cdot \text{Br}\cdot \text{Cl}_2\cdot 32\text{H}_2\text{O}$ (3): C, 44.18; H, 6.50; N, 18.67. Found: C, 44.27; H, 4.45; N, 18.76.

Isothermal Titration Calorimetry (ITC) Experiments. All titrations were carried out on a ITC instrument and repeated three times. All solutions were prepared in purified water and degassed prior to titration experiments. An aqueous solution (0.1 mM) of MeV^{2+} or EV^{2+} was placed in the sample cell (1.3 mL). The solution of the host Cy6CB6 (1.0 mM) was added in a series of 25 injections (10 μL). The heat evolved was recorded at $T = 298.15$ K. Computer simulations (curve fitting) were performed using the ITC software. The first data point was always removed from the data set prior to curve fitting. The data were analyzed with ORIGIN 8.0 software using the independent model.

Crystal Structure Determination. Single-crystal X-ray data were collected on a computer-controlled CCD diffractometer equipped with a graphite-monochromated Mo $\text{K}\alpha$ radiation ($\lambda = 0.71073$ Å).

Absorption corrections were applied by using the multiscan program SADABS. The structures were solved by direct methods and refined on F^2 using the SHELXL-97 crystallographic package.²⁰ All the non-hydrogen atoms were refined anisotropically. The carbon-bound hydrogen atoms were introduced at calculated positions. For solid compounds 2 and 3, the SQUEEZE process in the PLATON software program was applied to remove some bromide anions and water molecules because they could not be satisfactorily modeled.²¹

ASSOCIATED CONTENT

Supporting Information

The Supporting Information is available free of charge on the ACS Publications website at DOI: 10.1021/acs.joc.5b01557.

NMR spectroscopic data (2D COSY) for guest HV^{2+} and its inclusion complex, Cy6CB6· HV^{2+} (PDF)

Crystallographic data for compound 1 (CIF)

Crystallographic data for compound 2 (CIF)

Crystallographic data for compound 3 (CIF)

AUTHOR INFORMATION

Corresponding Authors

*E-mail: jxliu411@ahut.edu.cn

*E-mail: akaifer@miami.edu

Notes

The authors declare no competing financial interest.

ACKNOWLEDGMENTS

The authors are grateful to the National Science Foundation (to A.E.K., CHE-1412455) for the generous support of this work. J.-X.L. acknowledges the support from the Chinese Scholarship Council and the National Natural Science Foundation of China (21371004).

REFERENCES

- Lee, J. W.; Samal, S.; Selvapalam, N.; Kim, H.-J.; Kim, K. *Acc. Chem. Res.* **2003**, *36*, 621–630.
- Lagona, J.; Mukhopadhyay, P.; Chakrabarti, S.; Isaacs, L. *Angew. Chem., Int. Ed.* **2005**, *44*, 4844–4870.
- Isaacs, L. *Chem. Commun.* **2009**, 619–629.
- Kim, K.; Selvapalam, N.; Ko, Y. H.; Park, K. M.; Kim, D.; Kim, J. *Chem. Soc. Rev.* **2007**, *36*, 267–279.
- Ni, X. L.; Xiao, X.; Cong, H.; Liang, L. L.; Cheng, K.; Cheng, X. J.; Ji, N. N.; Zhu, Q. J.; Xue, S. F.; Tao, Z. *Chem. Soc. Rev.* **2013**, *42*, 9480–9508.
- Masson, E.; Ling, X.; Joseph, R.; Kyeremeh-Mensah, L.; Lu, X. *RSC Adv.* **2012**, *2*, 1213–1247.
- Isaacs, L. *Acc. Chem. Res.* **2014**, *47*, 2052–2062.
- Kaifer, A. E. *Acc. Chem. Res.* **2014**, *47*, 2160–2167.
- Zhao, Y. J.; Xue, S. F.; Zhu, Q. J.; Tao, Z.; Zhang, J. X.; Wei, Z. B.; Long, L. S.; Hu, M. L.; Xiao, H. P.; Day, A. I. *Chin. Sci. Bull.* **2004**, *49*, 1111–1116.
- Kim, Y.; Kim, H.; Ko, Y. H.; Selvapalam, N.; Rekharsky, M. V.; Inoue, Y.; Kim, K. *Chem. - Eur. J.* **2009**, *15*, 6143–6151.
- Feng, X.; Li, Z. F.; Xue, S. F.; Tao, Z.; Zhu, Q. J.; Zhang, Y. Q.; Liu, J. X. *Inorg. Chem.* **2010**, *49*, 7638–7640.
- Qin, X.; Ni, X. L.; Hu, J. X.; Chen, K.; Zhang, Y. Q.; Redshaw, C.; Zhu, Q. J.; Xue, S. F.; Tao, Z. *CrystEngComm* **2013**, *15*, 738–744.
- Kim, H. J.; Jeon, W. S.; Ko, Y. H.; Kim, K. *Proc. Natl. Acad. Sci. U. S. A.* **2002**, *99*, 5007–5011.
- Ong, W.; Gómez-Kaifer, M.; Kaifer, A. E. *Org. Lett.* **2002**, *4*, 1791–1794.
- Khan, M. S. A.; Heger, D.; Necas, M.; Sindelar, V. *J. Phys. Chem. B* **2009**, *113*, 11054–11057.
- Xiao, X.; Hu, Q. H.; Tao, Z.; Zhang, Y. Q.; Xue, S. F.; Zhu, Q. J.; Wei, G. *Chem. Phys. Lett.* **2011**, *514*, 317–320.

- (17) Kolman, V.; Khan, M. S. A.; Babinsky, M.; Marek, R.; Sindelar, V. *Org. Lett.* **2011**, *13*, 6148–6151.
- (18) Wittenberg, J. B.; Zavalij, P. Y.; Isaacs, L. *Angew. Chem., Int. Ed.* **2013**, *52*, 3690–3694.
- (19) Moon, K.; Kaifer, A. E. *Org. Lett.* **2004**, *6*, 185–188.
- (20) Sheldrick, G. M. *Acta Crystallogr., Sect. A: Found. Crystallogr.* **2008**, *64*, 112–122.
- (21) Spek, A. L. *J. Appl. Crystallogr.* **2003**, *36*, 7–13.